Int. J. Solids Structures Vol. 24, No. 2, pp. 139–151, 1988
Printed in Great Britain.

0020–7683/88 $3.00+ .00
© 1988 Pergamon Journals Ltd.

A TORSION LOAD TRANSFER PROBLEM FOR A CLASS OF NON-HOMOGENEOUS ELASTIC SOLIDS

R. K. N. D. Rajapakse
Department of Civil Engineering, University of Manitoba, Winnipeg, Canada R3T 2N2

(*Received* 24 *March* 1987; *in revised form* 2 *July* 1987)

Abstract—This paper is concerned with the axisymmetric torsion of a finite (long) cylindrical bar which is partially embedded in a non-homogeneous transversely isotropic elastic layer underlaid by a rigid base. The non-homogeneity of the elastic layer is represented by both linear and non-linear variations of shear moduli with depth. The bar–elastic layer system is decomposed to a real bar and an elastic layer with a cylindrical cavity identical to the embedded bar, instead of adopting the conventional fictitious bar-extended elastic medium decomposition. The proposed decomposition allows the imposition of displacement compatibility and traction continuity along the true contact surface in the analysis. A solution scheme based on a classical variational theorem is presented to analyse the load transfer problem. The displacement and traction Green's functions of the non-homogeneous elastic layer are required in the analysis and these are derived explicitly using Hankel integral transforms. Numerical results are presented to illustrate the effect of non-homogeneity and transverse isotropy on the torque twist relationship at the top end of the bar and twist angle and torque transfer curves along the length of the bar.

INTRODUCTION

The boundary-value problem involving a statically loaded elastic cylindrical bar partially embedded in an elastic medium has useful applications in several branches of engineering. A review of existing literature reveals that the analytical study of the torsional load transfer problem has received some attention. Freeman and Keer (1967) and Keer and Freeman (1970) presented exact analytical formulations for torsion of a finite elastic rod welded to the free surface of an elastic half-space and that for an infinitely long elastic rod with a finite protruding length and embedded in a homogeneous isotropic half-space, respectively. The torsional load transfer problem involving a finite elastic cylinder partially embedded in a layered elastic half-space has been considered by Karasudhi *et al.* (1984) by using the solution approach presented by Muki and Sternberg (1970) for the axial load transfer problem. A solution was presented (Selvadurai and Rajapakse, 1987) based on the decomposition proposed by Muki and Sternberg (1970) and a variational method to solve the torsional load-transfer problem. In addition Poulos (1975) presented an approximate solution using the finite difference technique and Randolph (1981) analysed the torsional load transfer problem using a simplified representation of the stress field in the surrounding half-space.

Load transfer studies available at present are based on the idealization that the surrounding elastic medium is homogeneous or layered and isotropic. However, for applications in geomechanics such an idealization is contrary to the fact that the shear modulus of the surrounding medium varies continuously with depth according to the geologic and loading history of the soil deposit (Wroth *et al.*, 1984). In addition, experimental investigation of natural soil deposits confirms the presence of anisotropy. The incorporation of both non-homogeneity and anisotropy into the load transfer analysis would enhance the practicality of the solution and its usefulness to engineering practice. Furthermore, a rigorous treatment of non-homogeneity and anisotropy would lead to a proper quantification of the influence of these factors on the solution and serve as the basis for comparison of approximate schemes (Randolph, 1981) and finite element solutions. In general studies involving non-homogeneous elastic media are rather limited. The complexity of the problem is such that only a few boundary-value problems involving surface loading of a non-homogeneous half-space have been considered (Kassir, 1970; Chuaprasert and Kassir, 1973; Erguven, 1982; Selvadurai *et al.*, 1986).

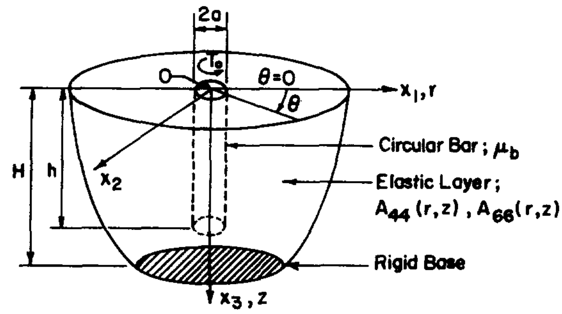

Fig. 1. Elastic bar embedded in non-homogeneous transversely isotropic elastic layer.

The torsional load transfer problem considered in this study is shown in Fig. 1. The surrounding medium is modelled as a non-homogeneous transversely isotropic elastic layer of finite thickness overlying a rigid base. The variation of shear moduli with depth is represented by two types of non-linear functions. In the present study the general solution for axisymmetric torsional displacement and stresses in a non-homogeneous transversely isotropic elastic solid is obtained through the application of Hankel integral transform techniques. The general solution is used to derive displacement and traction Green's functions corresponding to a concentrated ring load in the θ-direction acting in the interior of the elastic layer. The bar–elastic medium system is decomposed to a real bar and an elastic layer with a cavity identical to the bar. This decomposition allows the imposition of displacement compatibility and traction continuity along the true contact surface between the bar and the surrounding medium.

The displacement of the real bar is represented by an admissible function containing a set of generalized coordinates which is consistent with the assumed one-dimensional behaviour. A total potential energy functional is developed for the bar–elastic medium system in terms of generalized coordinates. The energy functional also involves a relationship between traction and displacement along the surface of the cylindrical cavity in the elastic layer. This relationship is established with respect to a set of discrete points on the cavity surface using the derived traction and displacement Green's functions of the undisturbed elastic layer. A minimization of total potential energy functional results in a linear simultaneous equation system for determination of generalized coordinates. The numerical study presented in this paper intends to portray the significance of non-homogeneity, transverse isotropy and bar flexibility on the torque–twist relationship at the top end of the bar and twist angle and torque transfer curves along the length of the bar.

GENERAL SOLUTION AND GREEN'S FUNCTIONS

In the present study the cylindrical polar coordinate system (r, θ, z) is adopted with the z-axis normal to the free surface of the elastic layer as shown in Fig. 1. Due to the axially symmetric nature of the problem under consideration the stresses and displacements are independent of the θ-coordinate and only the displacement $v(r, z)$ in the θ-direction exists. It should be mentioned here that axially symmetric deformation fields are possible only for a limited form of anisotropy such as the case of transverse isotropy. The relationship between the non-zero stress components and displacement $v(r, z)$ is obtained from the generalized Hooke's law (Lekhnitskii, 1963) as

$$\sigma_{\theta z} = A_{44}(r,z)\frac{\partial v}{\partial z}\,; \quad \sigma_{r\theta} = A_{66}(r,z)\left(\frac{\partial v}{\partial r} - \frac{v}{r}\right) \tag{1}$$

where

$$A_{66} = (A_{11}-A_{12})/2. \tag{2}$$

In eqns (1) and (2) $A_{ij}(r,z)$ denote a modulus of elasticity appearing in the generalized Hooke's law (Lekhnitskii, 1963). Coefficients A_{44} and A_{66} could be physically interpreted as the shear moduli for the planes parallel and perpendicular to the z-axis, respectively. At this stage it is convenient to non-dimensionalize the entire problem including the coordinate frame by defining "a" which denotes the radius of the embedded bar as a unit length.

The governing equation for the present class of problems in the absence of body forces could be expressed as

$$\frac{\partial}{\partial r}\left[A_{66}\left(\frac{\partial v}{\partial r}-\frac{v}{r}\right)\right]+\frac{\partial}{\partial z}\left[A_{44}\frac{\partial v}{\partial z}\right]+\frac{2A_{66}}{r}\left(\frac{\partial v}{\partial r}-\frac{v}{r}\right)=0. \tag{3}$$

For most applications in geomechanics shear moduli of natural soil deposits increase with depth due to the increase in effective overburden pressure and degree of over-consolidation. In addition the homogeneous condition could be justified in the radial direction. Under these assumptions shear moduli A_{44} and A_{66} are functions of the z-coordinate only. It is also assumed that the ratio of shear moduli A_{44} and A_{66} is spatially independent.

The shear moduli of the surrounding medium is assumed to vary with depth according to the following functional forms.

$$A_{44}(z) = \mu_0(1+mz)^{\alpha} \tag{4a}$$

or

$$A_{44}(z) = \mu_0\, e^{\beta z} \tag{4b}$$

$$A_{66}(z) = \gamma A_{44}(z), \quad \gamma > 0. \tag{4c}$$

In eqns (4), $\alpha = \beta = 0$ represents a homogeneous transversely isotropic solid; $\alpha > 0$ or $\beta > 0$ represents a situation where shear moduli increase non-linearly with depth; $\alpha < 0$ or $\beta < 0$ represents a situation where shear moduli decrease with depth and $\alpha = 1$ corresponds to an elastic medium with linearly increasing shear moduli. The constant γ is a measure of transverse isotropy and $\gamma = 1$ represents an isotropic solid. It is evident that eqns (4) could represent a variety of practical situations.

The general solution of eqn (3) could be obtained through the application of Hankel integral transforms. Following Sneddon (1951) the displacement $v(r,z)$ in the θ-direction is taken in the form

$$v(r,z) = \int_0^{\infty} F(\xi,z)J_1(\xi r)\, d\xi. \tag{5}$$

In eqn (5), J_1 denotes the Bessel function of the first kind and first order. Substitution of eqn (5) into eqn (3) and considering the appropriate variation of shear modulus as given by eqn (4a) or (4b) together with eqn (4c) leads to the following general solution for displacement $v(r,z)$ in the θ-direction:

$$v(r,z) = \int_0^{\infty} [C(\xi)\, e^{c_1 z}+D(\xi)\, e^{c_2 z}]J_1(\xi r)\, d\xi \quad \text{for} \quad A_{44}(z) = \mu_0\, e^{\beta z} \tag{6}$$

where

$$c_1 = \frac{-\beta-(\beta^2+4\xi^2\gamma)^{1/2}}{2} \quad \text{and} \quad c_2 = \frac{-\beta+(\beta^2+4\xi^2\gamma)^{1/2}}{2}$$

$$v(r,z) = (\bar{m}+z)^p\gamma^{p/2}\int_0^\infty \{C(\xi)I_p[(\bar{m}+z)\xi\gamma^{1/2}]+D(\xi)K_p[(\bar{m}+z)\xi\gamma^{1/2}]\}J_1(\xi r)\,\mathrm{d}\xi$$

$$\text{for} \quad A_{44}(z) = \mu_0(1+mz)^\alpha \quad (7)$$

where

$$2p = 1-\alpha; \quad \bar{m} = 1/m.$$

In eqns (6) and (7), $C(\xi)$ and $D(\xi)$ are arbitrary functions which should be determined by invoking appropriate boundary and continuity conditions; I_p and K_p in eqn (7) denote modified Bessel functions of the first and second kind of order p, respectively. For a domain which extends to infinity in the z-direction in order to satisfy regularity conditions of displacement and stresses, general solutions represented by eqns (6) and (7) reduce to the following expressions:

$$v(r,z) = \int_0^\infty C(\xi)\,\mathrm{e}^{c_1 z}\,J_1(\xi r)\,\mathrm{d}\xi \quad (8)$$

$$v(r,z) = (\bar{m}+z)^p\gamma^{p/2}\int_0^\infty D(\xi)K_p[(\bar{m}+z)\xi\gamma^{1/2}]J_1(\xi r)\,\mathrm{d}\xi \quad (9)$$

In the ensuing section dealing with the variational formulation of the load transfer problem a relationship between a traction field in the θ-direction applied over the surface of a cylindrical cavity created in the non-homogeneous elastic layer and the corresponding displacement in the θ-direction is required. A discrete version of this relationship in terms of a set of nodal points located on the cavity surface could be established through displacement and traction Green's functions corresponding to an undisturbed (without a cavity) non-homogeneous elastic layer. The relevant Green's functions could be derived by utilizing eqns (1), (6)–(9) and following the procedure similar to that adopted for a homogeneous medium (Karasudhi *et al.*, 1984; Selvadurai and Rajapakse, 1987). The displacement Green's functions $G_{\theta\theta}(r,z;s,z')$ denoting the displacement in the θ-direction at point (r,z) due to a unit ring load through the point (s,z') is presented explicitly in the Appendix. The traction Green's function $H_{\theta\theta}(r,z;s,z')$ could be obtained from $G_{\theta\theta}$ using basic relationships in elasticity (Fung, 1965). The relevant expression for $H_{\theta\theta}$ in terms of $G_{\theta\theta}$ is given by eqn (A14) in the Appendix.

VARIATIONAL FORMULATION OF TORSION LOAD TRANSFER PROBLEM

Consider a cylindrical elastic bar with radius a and length $h(h/a \gg 1)$ embedded in a non-homogeneous transversely isotropic elastic layer overlying a rigid base as shown in Fig. 1. The bar is perfectly bonded to the surrounding elastic layer along the shaft ($r = a$, $0 \leqslant z \leqslant h$) and the base ($z = h$, $0 \leqslant r \leqslant a$). The thickness of the elastic layer is denoted by H and variation of shear moduli A_{44} and A_{66} with depth is defined according to eqns (4). The embedded bar consists of a homogeneous isotropic elastic material the shear modulus of which is denoted by μ_b. The bar which is flushed at the free surface level is subjected to a torque T_0 at $z = 0$ and under this loading configuration experiences a rotation ϕ_0 at the top end.

In the present study a novel solution scheme which is based on the decomposition of the bar–elastic medium system into an elastic medium $\bar{\mathbf{B}}$ with a cylindrical cavity identical

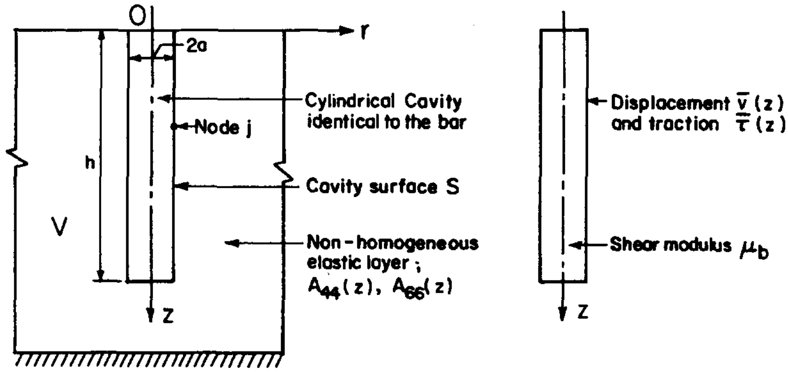

Fig. 2. Decomposition of bar–elastic layer system: (a) elastic layer with cylindrical cavity $\bar{B}$; (b) real elastic bar B.

to the bar and the real bar B as shown in Fig. 2 is presented to analyse the title problem. In view of this decomposition, the load transfer problem could be formulated on the basis of displacement compatibility and traction continuity on the true contact surface between the bar and the surrounding medium instead of treating fictitious systems (Karasudhi *et al.*, 1984; Selvadurai and Rajapakse, 1987). Furthermore, the consideration of anisotropy of any type in a strict sense does not allow the decomposition originally proposed by Muki and Sternberg (1970). In the following anslysis $\bar{B}$ and B are treated using three- and one-dimensional theory, respectively.

The assumption that the bar is governed by a one-dimensional theory enables the only non-vanishing displacement v_b in the θ-direction of the real bar to be expressed in the admissible form

$$v_b(r,z) = \sum_{n=1}^{N} b_n \psi_n(r,z). \tag{10}$$

In eqn (10), b_n could be viewed as a set of generalized coordinates and the number of terms N to be decided by a convergence study. The functions $\psi_n(r,z)$ may be selected as

$$\psi_n(r,z) = r\,\mathrm{e}^{-(n-1)z/h}. \tag{11}$$

In view of eqns (10) and (11), the strain energy U_b of the elastic bar B can be expressed as

$$U_b = \sum_{n=1}^{N}\sum_{m=1}^{N} b_n b_m D_{mn} \tag{12}$$

where

$$\begin{aligned} D_{mn} &= \frac{\pi\mu_b}{4h}\frac{(m-1)(n-1)}{(m+n-2)}(1-\mathrm{e}^{-(m+n-2)}); \quad m+n \neq 2 \\ &= 0 \quad \text{for} \quad m+n = 2. \end{aligned} \tag{13}$$

The strain energy U_L of the elastic layer $\bar{B}$ with the cavity could be expressed as

$$\begin{aligned} U_L &= \frac{1}{2}\int_V (\sigma_{r\theta}\varepsilon_{r\theta} + \sigma_{z\theta}\varepsilon_{z\theta})\,\mathrm{dV} \\ &= \frac{1}{2}\int_S \bar{\tau}\bar{v}\,\mathrm{dS}. \end{aligned} \tag{14}$$

In eqn (14), $\bar{v}$ denotes the displacement on S as given by eqn (10). The traction $\bar{\tau}$ in the θ-direction on S corresponds to displacement $\bar{v}$. In view of eqn (10)

$$\bar{v} = \sum_{n=1}^{N} b_n \bar{v}_n \tag{15a}$$

where

$$\bar{v}_n = \psi_n(r, z), \quad (r, z) \in \mathrm{S}. \tag{15b}$$

The traction $\bar{\tau}$ could be written as

$$\bar{\tau} = \sum_{n=1}^{N} b_n \bar{\tau}_n \tag{16}$$

where $\bar{\tau}_n$ is the traction on S due to the displacement field $\bar{v}_n$ imposed on S.

The solution of the mixed-boundary value problem corresponding to domain $\bar{\mathrm{B}}$ to determine $\bar{\tau}_n$ due to $\bar{v}_n$ imposed on S is not straightforward. In fact it is impossible to obtain an explicit representation of $\bar{\tau}_n$ for the $\bar{v}_n$ given by eqn (15b). The application of integral representation theorems for an elastic solid (Eringen and Suhubi, 1975) to $\bar{\mathrm{B}}$ leads to a relationship between $\bar{\tau}_n$ and $\bar{v}_n$ expressed in the form of an integral equation on S. Therefore, it is possible to write the following matrix relationship involving values of $\bar{\tau}_n$ and $\bar{v}_n$ at a set of nodal locations selected on S:

$$\{\bar{\tau}_{nj}\} = [K]\{\bar{v}_{nj}\}. \tag{17}$$

In eqn (17), $\bar{\tau}_{nj}$ and $\bar{v}_{nj}$ denote traction in the θ-direction and displacement in the θ-direction at node j on S and a total of M nodes is used to discretize S. The determination of matrix $[K]$ of size $M \times M$ will be discussed in the ensuing section. In view of eqns (14)–(16), U_{L} can be expressed as

$$U_{\mathrm{L}} = \frac{1}{2} \sum_{m=1}^{N} \sum_{n=1}^{N} \sum_{j=1}^{M} b_n b_m \bar{\tau}_{nj} \psi_{mj} A_j. \tag{18}$$

In eqn (18), A_j is the tributary area corresponding to node j on S and ψ_{mj} is given by eqn (11) when applied to nodes.

The total potential energy functional χ for the bar–elastic layer system can be written as (Washishu, 1982)

$$\chi = U_{\mathrm{L}} + U_{\mathrm{b}} - T_0 \sum_{n=1}^{N} b_n \psi_n(1, 0). \tag{19}$$

The minimization of eqn (19) with respect to generalized coordinates b_n yields

$$\sum_{n=1}^{N} b_n \left[2D_{ni} + \sum_{j=1}^{M} (\bar{\tau}_{nj}\psi_{ij} + \bar{\tau}_{ij}\psi_{nj}) A_j / 2 \right] = T_0 \quad (i = 1, 2, \ldots, N). \tag{20}$$

The numerical solution of eqn (20) for a given bar–elastic layer system results in the solution for b_n ($n = 1, \ldots, N$). Thereafter eqn (10) could be used to compute the displacement (twist) profile along the bar length. The resultant torque $T(z)$ acting on the bar at a depth z can be determined from the following equations:

$$T(z) = \mu_{\mathrm{b}} J \sum_{n=1}^{N} b_n \psi'_n(1, z) \tag{21}$$

where

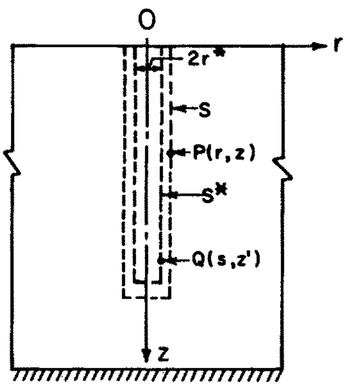

Fig. 3. Uniform non-homogeneous elastic layer B* used to derive [K].

$$\psi_n'(1,z) = \frac{d\psi_n(1,z)}{dz}, \quad J = \frac{\pi}{2}. \tag{22}$$

It is interesting to note the simplicity of eqns(10) and (21) which represent expressions for angle of twist, and torque diffusion along the bar length when compared to corresponding expressions in Karasudhi *et al.* (1984) involving complicated integral equations with kernels consisting of infinite integrals of the Lipschitz–Hankel type (Eason *et al.*, 1955). In addition to these advantages the compatibility condition employed in the present formulation is more realistic and the deformation of the real bar is totally consistent with the assumed one-dimensional behaviour.

TRACTION–DISPLACEMENT RELATIONSHIP ALONG CAVITY SURFACE

The successful implementation of the present formulation depends on the determination of [K] in eqn (17) which determines $\bar{\tau}_n$ on S for a specified $\bar{v}_n$ on S. In the present study, the indirect traction method by Ohsaki (1973) to study the movement of a rigid body embedded in an elastic half-space is applied to determine [K]. In this method a uniform non-homogeneous elastic layer B* without a cavity as shown in Fig. 3 is considered. The contour S representing the true contact surface is also defined in B*. Interior to S, an arbitrary surface S* with geometry similar to S is defined. A traction field τ_n^* in the θ-direction is applied on S* such that the displacement in the θ-direction on S is equal to $\bar{v}_n$. Under this condition the following non-singular integral equation can be established:

$$\bar{v}_n(r,z) = \int_{S^*} G_{\theta\theta}(r,z;s,z')\tau_n^*(s,z')\, dS^*, \quad (r,z) \in s, \quad (s,z') \in S^*. \tag{23}$$

In eqn (23), $G_{\theta\theta}(r,z;s,z')$ is the displacement Green's function for B* which is explicitly presented by eqns (A1)–(A13) in the Appendix. Alternatively, a discrete representation of eqn (23) with respect to a set of nodal points on S* and S can be written as

$$[\bar{G}_{ij}]\{\tau_{nj}^*\} = \{\bar{v}_{ni}\} \tag{24}$$

where

$$\bar{v}_{ni} = \bar{v}_n(r_i, z_i) \quad (r_i, z_i) \in S$$
$$\tau_{nj}^* = \tau_n^*(s_j, z_j') \quad (s_j, z_j') \in S^*$$
$$\bar{G}_{ij} = G_{\theta\theta}(r_i, z_i; s_j, z_j')A_j^*$$
$$A_j^* = \text{Tributary area for node } j \text{ on } S^*.$$

In general the total number of nodes M^* on S* and M on S need not be equal and eqn (24) could be solved for $\{\tau^*_{nj}\}$ in a least square sense. This leads to

$$\{\tau^*_{nj}\} = [[\bar{G}]^T[\bar{G}]]^{-1}[\bar{G}]^T\{\bar{v}_{nj}\}. \tag{25}$$

Since the displacement on S is $\bar{v}_n$ the corresponding traction $\bar{\tau}_n$ is given by the following non-singular integral equation:

$$\bar{\tau}_n(r,z) = \int_{S^*} H_{\theta\theta}(r,z;s,z')\tau^*_n(s,z')\ \mathrm{d}S^*. \tag{26}$$

Alternatively

$$\{\bar{\tau}_{ni}\} = [\bar{H}_{ij}]\{\tau^*_{nj}\} \tag{27}$$

where

$$\bar{H}_{ij} = H_{\theta\theta}(r_i, z_i; s_j, z'_j)A^*_j. \tag{28}$$

In eqn (26), $H_{\theta\theta}(r,z;s,z')$ denotes the traction in the θ-direction on a plane with unit normal **n** through a point (r,z) on S due to a unit ring load in the θ-direction through point (s,z') on S*. Note $H_{\theta\theta}$ is related to $G_{\theta\theta}$ as given by eqn (A14) in the Appendix.

In view of eqns (27) and (25)

$$\{\bar{\tau}_{nj}\} = [\bar{H}]\,[[\bar{G}]^T[\bar{G}]]^{-1}[\bar{G}]^T\{\bar{v}_{nj}\}. \tag{29}$$

Comparison of eqns (17) and (29) leads to

$$[K] = [\bar{H}]\,[[\bar{G}]^T[\bar{G}]]^{-1}[\bar{G}]^T. \tag{30}$$

Therefore, eqn (30) together with the explicit representations of Green's functions $G_{\theta\theta}$ and $H_{\theta\theta}$ given in the Appendix make $[K]$ fully determinate for a given problem.

NUMERICAL RESULTS AND DISCUSSION

The major computational effort in the numerical study is associated with the evaluation of Green's functions $G_{\theta\theta}$ and $H_{\theta\theta}$ required to establish $[K]$ given by eqn (30). These Green's functions consisting of infinite integrals are computed using an appropriate numerical integration scheme with due consideration given to the oscillating nature of the integrand. The variation of non-dimensionalized torsional stiffness K_T ($K_T = 3T_0/16\mu_0 a^3\phi_0$) for different discretizations adopted for S and S* and location of S* characterized by radius r^* (Fig. 3) is presented in Table 1. The convergence of solution is clearly evident and more complete comparisons involving twist and torque transfer profiles along the bar length were also made to confirm the convergence. These solutions are not presented for brevity. The

Table 1. Variation of non-dimensionalized stiffness K_T with discretizations adopted for S and S*, $h/a = 10$, $\beta = 0.2$, $\gamma = 1.5$, $H/a = 15.0$, $N = 8$

	$\bar{\mu} = 50$		$\bar{\mu} = 2000$	
(M, M^*)	$r^* = 0.85$	$r^* = 0.90$	$r^* = 0.85$	$r^* = 0.9$
(12, 8)	7.74	7.38	57.96	56.83
(18, 12)	8.07	7.87	60.89	60.33
(25, 20)	8.47	8.43	62.78	63.10
(35, 30)	8.48	8.45	63.27	63.54
(40, 30)	8.50	8.49	63.26	63.70

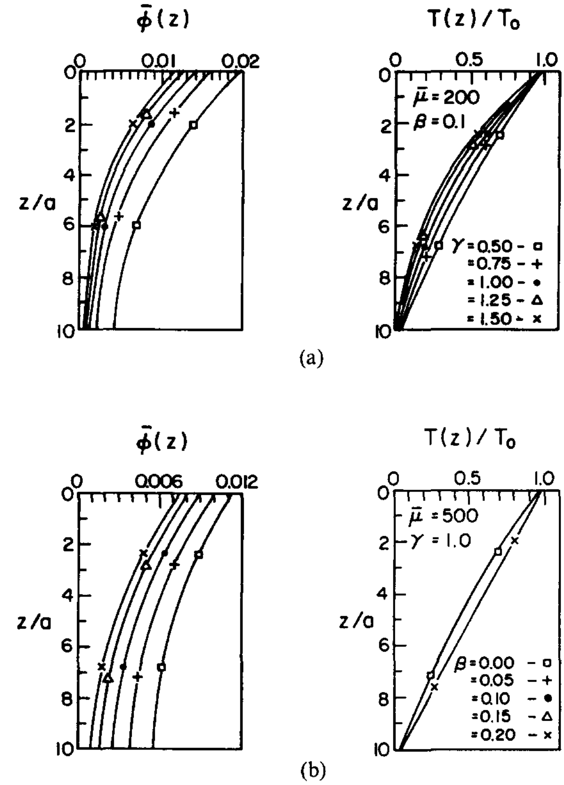

Fig. 4. Twist and torque profiles for elastic bar embedded in a medium where $A_{44} = \mu_0 \, e^{\beta z}$; $h/a = 10$, $M = 30$, $M^* = 20$, $r^* = 0.85$, $H/a = 20$: (a) variation of twist and torque profiles with γ; (b) variation of twist and torque profiles with β.

convergence of the numerical solution with the total number of terms (N) used to represent bar deformation field in eqn (10) was also investigated and sufficient convergence was observed for $N \geqslant 6$.

The influence of the layer thickness (H) on numerical solutions was investigated by considering a rigid bar with $h/a = 10$. Note that the solution corresponding to the base of a rigid bar represents the situation where the influence of layer thickness is most significant. Numerical solutions for base twist and base torque were found to change about 5 and 15% when H/a is changed from 10.5 to 20.0, respectively. In general, for $(H-h)/a > 2.0$ the thickness of the layer was found to have negligible influence. This is not surprising since the classical Reissner–Sagoci problem indicates that stresses and displacements at depths greater than twice the plate radius are quite negligible.

Figure 4(a) shows the influence of the transverse isotropy parameter γ on the non-dimensionalized twist angle $\bar{\phi}(z)$ ($\bar{\phi}(z) = \phi(z)\mu_0 a^3/T_0$) and bar torque $T(z)$ along the length of an elastic bar with $\bar{\mu} = 200$ ($\bar{\mu} = \mu_b/\mu_0$), embedded in a non-homogeneous medium represented by eqn (4b) with $\beta = 0.1$. Comparison of solutions corresponding to $\gamma = 1.0$ (isotropic) with those corresponding to other γ values shows the significance of transverse isotropy in the torsion load transfer problem. The influence of the non-homogeneity parameter β on the torque and twist profiles are presented in Fig. 4(b) for an elastic layer which is isotropic ($\gamma = 1$) and for a bar with $\bar{\mu} = 500$. The significance of non-homogeneity is clearly evident on the twist angle but the torque transfer profiles show less dependence on β. This behaviour could be interpreted from the shape of twist angle profiles since the resultant torque at the bar cross-section is directly proportional to the slope of the twist angle profile at a given depth.

The influence of non-homogeneity of the form $A_{44}(z) = \mu_0(1+mz)^\alpha$ on the torsion load-transfer problem is depicted in Fig. 5. The torque and twist angle profiles corresponding to a bar with $\bar{\mu} = 200$ embedded in a surrounding medium which is isotropic and has linearly increasing shear modulus with depth ($\alpha = 1$) is shown in Fig. 5(a) for different

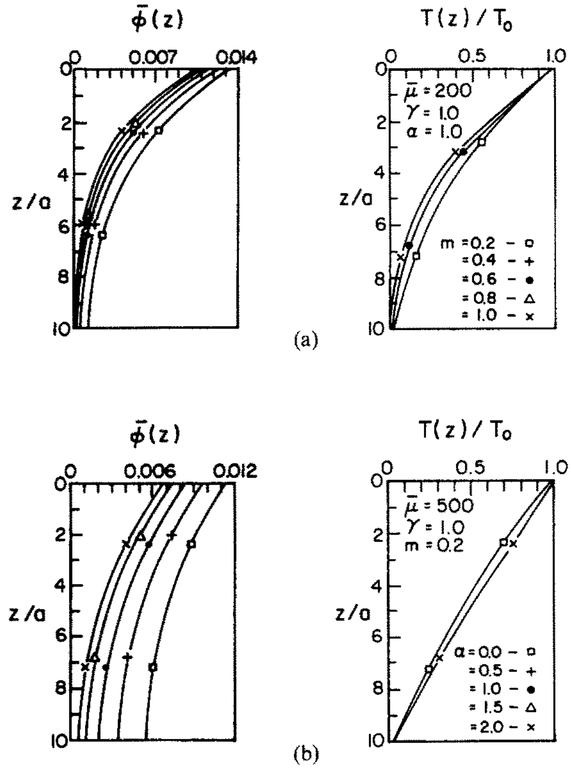

Fig. 5. Twist and torque profiles for elastic bar embedded in a medium where $A_{44} = \mu_0(1+mz)^\alpha$; $h/a = 10$, $M = 30$, $M^* = 20$, $r^* = 0.85$, $H/a = 20$: (a) variation of twist and torque profiles with parameter m; (b) variation of twist and torque profiles with α.

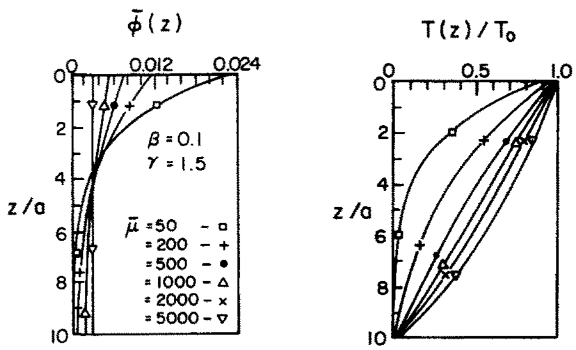

Fig. 6. Twist and torque profiles for various values of bar flexibility ratio $\bar{\mu}$; $h/a = 10$, $M = 30$, $M^* = 20$, $r^* = 0.85$, $H/a = 20$.

values of m. These results indicate that as the gradient m of the shear modulus variation increases the system becomes stiffer and twist angle decreases sharply along the length. The torque transfer profiles show more diffusion of torque in the central region of the bar with increasing values of m. The significance of parameter α which reflects the non-linearity of shear moduli with depth is investigated in Fig. 5(b) for a bar with $\bar{\mu} = 500$ embedded in an isotropic half-space with $m = 0.2$. The solution corresponding to a surrounding isotropic ($\gamma = 1$) and homogeneous medium ($\alpha = 0$) is also plotted in Fig. 5(b). The influence of parameter α on the twist profile is clearly evident and the behaviour of torque transfer profiles is similar to that observed for variations of the non-homogeneity index β in Fig. 4(b). The relative insignificance of α on torque transfer profiles is evident since the slope of twist angle profiles are nearly identical for different values of α. However, in a separate numerical study it was observed that as the bar becomes stiffer the torque transfer curves show a more significant influence of parameter α.

The significance of shear moduli ratio $\bar{\mu}$ on the torsion load transfer problem is shown in Fig. 6 for a bar with $h/a = 10.0$ embedded in an elastic medium where $\beta = 0.1$ and

Table 2. Variation of normalized stiffness $\bar{K}_T$ with bar flexibility, non-homogeneity parameter β and transverse isotropy index γ for a medium with $A_{44} = \mu_0 e^{\beta z}$; $h/a = 10$, $H/a = 20.0$, $M = 30$, $M^* = 20$, $r^* = 0.85$

	$\bar{K}_T$					
		$\beta = 0.1$			$\beta = 0.2$	
$\bar{\mu}$	$\gamma = 0.5$	$\gamma = 1.0$	$\gamma = 1.5$	$\gamma = 0.5$	$\gamma = 1.0$	$\gamma = 1.5$
10	0.73	1.03	1.27	0.76	1.07	1.31
50	0.77	1.06	1.29	0.83	1.13	1.36
100	0.79	1.09	1.32	0.88	1.18	1.41
200	0.82	1.14	1.38	0.95	1.27	1.50
500	0.86	1.27	1.56	1.13	1.52	1.79
1000	0.88	1.41	1.78	1.30	1.84	2.21
2000	0.90	1.54	2.03	1.48	2.26	2.80
50,000	0.92	1.77	2.56	1.84	3.38	4.81
∞	0.93	1.78	2.57	1.87	3.50	5.00

Table 3. Variation of normalized stiffness $\bar{K}_T$ with bar flexibility, non-homogeneity parameters m and α for a medium with $A_{44} = \mu_0(1+mz)^\alpha$; $h/a = 10$, $H/a = 20.0$, $M = 30$, $M^* = 20$, $r^* = 0.85$, $\gamma = 1.0$

	$\bar{K}_T$					
		$\alpha = 1.0$			$m = 0.2$	
$\bar{\mu}$	$m = 0.2$	$m = 0.6$	$m = 0.8$	$\alpha = 0.5$	$\alpha = 1.5$	$\alpha = 2.0$
10	1.06	1.16	1.21	1.03	1.09	1.13
50	1.11	1.26	1.32	1.05	1.16	1.22
100	1.15	1.33	1.40	1.07	1.22	1.29
200	1.21	1.44	1.52	1.10	1.30	1.39
500	1.36	1.73	1.85	1.18	1.54	1.70
1000	1.53	2.11	2.30	1.25	1.83	2.10
2000	1.71	2.61	2.92	1.31	2.17	2.66
50,000	2.04	4.06	5.05	1.41	3.00	4.47
∞	2.09	4.21	5.25	1.42	3.09	4.64

$\gamma = 1.5$. Numerical results presented in Fig. 6 correspond to the range $\bar{\mu} = 50$–5000 reflecting very flexible as well as nearly rigid bars. For flexible bars both twist and torque transfer profiles show a sharp decrease with depth. On the other hand as the bar becomes stiffer the twist angle approaches a constant value with depth and torque transfer profiles showing a more gradual diffusion of torque to the surrounding medium with depth.

In engineering applications of the present class of problems the quantity of interest is the torque–twist relationship K_T at the top end of the bar. The normalized stiffness $\bar{K}_T = K_T/K_0$, where K_0 is the K_T corresponding to an identical bar embedded in a homogeneous isotropic medium, is used in the present study instead of K_T to directly portray the significance of non-homogeneity and transverse isotropy on the global response of the system shown in Fig. 1. Solutions for K_0 are given in Karasudhi *et al.* (1984) and Selvadurai and Rajapakse (1987). The variation of $\bar{K}_T$ with bar flexibility, non-homogeneity parameter β and transverse isotropy index γ for a medium with $A_{44} = \mu_0 e^{\beta z}$ is presented in Table 2. Noting that $\gamma = 1.0$ represents an isotropic solid it is evident from these results that the transverse isotropy has a significant influence on the torsional stiffness for both very flexible and rigid bars. The influence of β for a given value of γ is relatively small for flexible bars since the torque diffusion is more rapid and only the top portion of the bar near the surface level is deformed. On the other hand as $\bar{\mu}$ increases the entire length of the bar undergoes deformations of the same order and torque transfer is more gradual and these characteristics increase in stiffness considerably for increasing values of β.

Table 3 presents the variation of $\bar{K}_T$ for an elastic bar embedded in an isotropic medium where non-homogeneity is represented by the form $A_{44}(z) = \mu_0(1+mz)^\alpha$. The first set of results (columns 2–4) correspond to a situation where shear modulus increases with depth linearly and gradient m is varied from 0.2 to 0.8. The general behaviour is similar to that observed in Table 2 for varying β. Numerical solutions are also presented in Table 3 for the case where $m = 0.2$ and α is varied from 0.5 to 2.0 to reflect a situation where the variation of shear moduli with depth is non-linear. The significance of α is clearly evident except for very flexible bars and the general trend is an increase in $\bar{K}_T$ with increasing α.

It can be concluded that an accurate solution algorithm based on a classical variational theorem and Green's functions for an undisturbed surrounding medium is presented to analyse the torsion load transfer from a long cylindrical elastic bar to a non-homogeneous transversely isotropic elastic layer. The analysis is based on a more realistic decomposition of the load transfer problem and satisfies the displacement compatibility and traction continuity on the true contact surface. The numerical study though not extensive reflects the significance of non-homogeneity, transverse isotropy and bar flexibility on the twist angle and torque transfer profiles along the bar length and on the torque–twist relationship at the top end of the bar. It is noted that the depth of the elastic layer has a negligible influence on the torsion load transfer problem if $(H-h)/a > 1.0$. The solution scheme presented in this paper could be directly used to analyse torsion transfer problems involving layered non-homogeneous media. In this case all Green's functions have to be constructed numerically since an explicit derivation is extremely tedious and impractical.

Acknowledgement—The work presented in this paper was supported by the Natural Sciences and Engineering Research Council of Canada, Grant A-6507.

REFERENCES

Chuaprasert, M. F. and Kassir, M. K. (1973). Torsion of non-homogeneous solid. *J. Engng Mech ASCE* **99**, 703–713.

Eason, E., Noble, B. and Sneddon, I. N. (1955). On certain integrals of Lipschitz–Hankel type involving products of Bessel functions. *Phil. Trans. R. Soc. London* **247**, 529–551.

Erguven, M. E. (1982). Torsion of a non-homogeneous transversely isotropic half-space. *Lett. Appl. Engng Sci.* **20**, 679.

Eringen, A. C. and Suhubi, E. H. (1975). *Elastodynamics*, Vol. 2. Academic Press, New York.

Freeman, N. J. and Keer, L. M. (1967). Torsion of a cylindrical rod welded to an elastic half-space. *J. Appl. Mech. ASME* **34**, 687–692.

Fung, Y. C. (1965). *Foundations of Solid Mechanics*. Prentice-Hall, Englewood Cliffs, New Jersey.

Karasudhi, P., Rajapakse, R. K. N. D. and Hwang, B. Y. (1984). Torsion of a long cylindrical elastic bar partially embedded in a layered elastic half space. *Int. J. Solids Structures* **20**, 1–11.

Kassir, M. K. (1970). The Reissner–Sagoci problem for a non-homogeneous solid. *Int. J. Engng Sci.* **8**, 875–885.

Keer, L. M. and Freeman, N. J. (1970). Load transfer problem for an embedded shaft in torsion. *J. Appl. Mech. ASME* **37**, 504–512.

Lekhnitskii, S. G. (1963). *Theory of Elasticity of an Anisotropic Elastic Body*. Holden-Day, San Francisco.

Muki, R. and Sternberg, E. (1970). Elastostatic load transfer to a half space from a partially embedded axially loaded rod. *Int. J. Solids Structures* **6**, 69–90.

Ohsaki, Y. (1973). On movements of a rigid body in semi-infinite elastic medium. *Proc. Japan Earthquake Engng Symp.*, Tokyo, Japan, pp. 245–252.

Poulos, H. G. (1975). Torsional response of piles. *J. Geotech. Engng Div. ASCE* **101**, 1019–1035.

Randolph, M. F. (1981). Piles subjected to torsion. *J. Geotech. Engng Div. ASCE* **107**, 1095–1111.

Selvadurai, A. P. S. and Rajapakse, R. K. N. D. (1987). A variational scheme for analysis of torsion of non-uniform elastic bars embedded in elastic media. *J. Engng Mech. Div. ASCE* **113**, 1534–1550.

Selvadurai, A. P. S., Singh, B. M. and Vrbik, J. (1986). A Reissner–Sagoci problem for a non-homogeneous elastic solid. *J. Elasticity* **16**, 383–391.

Sneddon, I. N. (1951). *Fourier Transforms*. McGraw-Hill, New York.

Washishu, K. (1982). *Variational Methods in Elasticity and Plasticity*, 3rd Edn. Pergamon Press, Oxford.

Wroth, C. P., Randolph, M. F., Houlsby, G. T. and Fahey, M. (1984). A review of the engineering properties of soils with particular reference to shear modulus. Soil Mech. Rept. No. SM049/84, University of Oxford.

APPENDIX

The expression for the displacement Green's function $G_{\theta\theta}(r, z; s, z')$ is given below.
For a medium with $A_{44}(z) = \mu_0 \, e^{\beta z}$

$$
\begin{aligned}
G_{\theta\theta}(r, z; s, z') &= \int_0^\infty \frac{(c_1 \, e^{c_2 z} - c_1 \, e^{c_1 z})}{c_1} D_1(\xi, z', H) G(s, r, \xi) \, d\xi \quad 0 \leqslant z \leqslant z' \\
&= \int_0^\infty (-e^{c_1 z + (c_2 - c_1) H} + e^{c_2 z}) D_2(\xi, z', H) G(s, r, \xi) \, d\xi \quad z' \leqslant z \leqslant H
\end{aligned}
\tag{A1}
$$

where

$$D_1(\xi, z', H) = \frac{c_1\,\mathrm{e}^{-c_2 z_1}\,(\mathrm{e}^{(c_2-c_1)H} - \mathrm{e}^{(c_2-c_1)z'})}{A_{44}(z')\,(c_2-c_1)\,(c_1\,\mathrm{e}^{(c_2-c_1)H} - c_2)} \tag{A2}$$

$$D_2(\xi, z', H) = \frac{(c_1\,\mathrm{e}^{-c_1 z'} - c_2\,\mathrm{e}^{-c_2 z'})}{A_{44}(z')\,(c_1-c_2)\,(c_1\,\mathrm{e}^{(c_2-c_1)H} - c_2)} \tag{A3}$$

$$G(s, r, \xi) = s\xi J_1(\xi s) J_1(\xi r). \tag{A4}$$

For the case of a non-homogeneous transversely isotropic half-space the expression for $G_{\theta\theta}(r, z; s, z')$ is reduced to the following form:

$$\begin{aligned} G_{\theta\theta}(r, z; s, z') &= \int_0^\infty \frac{[c_1\,\mathrm{e}^{c_2(z-z')} - c_2\,\mathrm{e}^{(c_1 z - c_2 z')}]}{c_1(c_2-c_1)A_{44}(z')} G(s, r, \xi)\,\mathrm{d}\xi \quad 0 \leqslant z \leqslant z' \\ &= \int_0^\infty \frac{[c_1\,\mathrm{e}^{c_1(z-z')} - c_2\,\mathrm{e}^{(c_1 z - c_2 z')}]}{c_1(c_2-c_1)A_{44}(z')} G(s, r, \xi)\,\mathrm{d}\xi \quad z' \leqslant z < \infty. \end{aligned} \tag{A5}$$

Note that c_1 and c_2 appearing in the above equations are defined under eqn (6).

For a medium with $A_{44}(z) = \mu_0(1+mz)^a$

$$\begin{aligned} G_{\theta\theta}(r, z; s, z') &= U^p \int_0^\infty [F(p-1, 0)I_p(U\xi) + K_p(U\xi)]D_1(\xi, z', H)\xi^{-1}G(s, r, \xi)\,\mathrm{d}\xi \quad 0 \leqslant z \leqslant z' \\ &= U^p \int_0^\infty [-F(p, H)I_p(U\xi) + K_p(U\xi)]D_2(\xi, z', H)\xi^{-1}G(s, r, \xi)\,\mathrm{d}\xi \quad z' \leqslant z \leqslant H \end{aligned} \tag{A6}$$

where

$$U = (\bar{m}+z)\gamma^{1/2} \tag{A7}$$

$$F(\beta, z) = K_\beta[(\bar{m}+z)\xi\gamma^{1/2}]/I_\beta[(\bar{m}+z)\xi\gamma^{1/2}] \tag{A8}$$

$$D_1(\xi, z', H) = -\frac{[F(p, H) - F(p, z')]}{A_{44}(z')I_{p-1}[(\bar{m}+z')\xi\gamma^{1/2}]\gamma^{1/2}[(\bar{m}+z')\gamma^{1/2}]^p}\,\frac{1}{[F(p, H)+F(p-1, 0)]\,[F(p, z')+F(p-1, z')]} \tag{A9}$$

$$D_2(\xi, z', H) = \frac{[F(p, z')+F(p-1, 0)]}{A_{44}(z')I_{p-1}[(\bar{m}+z')\xi\gamma^{1/2}]\gamma^{1/2}[(\bar{m}+z')\gamma^{1/2}]^p}\,\frac{1}{[F(p, H)+F(p-1, 0)]\,[F(p, z')+F(p-1, z')]}. \tag{A10}$$

For the case of a non-homogeneous transversely isotropic half-space with $A_{44}(z) = \mu_0(1+mz)^a$ the above expressions for $G_{\theta\theta}(r, z; s, z')$ reduces to the following form:

$$\begin{aligned} G_{\theta\theta}(r, z; s, z') &= U^p \int_0^\infty [F(p-1, 0)I_p(U\xi) + K_p(U\xi)]D_1(\xi, z')\xi^{-1}G(s, r, \xi)\,\mathrm{d}\xi \quad 0 \leqslant z \leqslant z' \\ &= U^p \int_0^\infty K_p(U\xi)D_2(\xi, z')\xi^{-1}G(s, r, \xi)\,\mathrm{d}\xi \quad z' \leqslant z < \infty \end{aligned} \tag{A11}$$

where

$$D_1(\xi, z') = \frac{F(p, z')}{A_{44}(z')I_{p-1}[(\bar{m}+z')\xi\gamma^{1/2}]\gamma^{1/2}[(\bar{m}+z')\gamma^{1/2}]^p}\,\frac{1}{F(p-1, 0)\,[F(p-1, z')+F(p, z')]} \tag{A12}$$

$$D_2(\xi, z') = \frac{[F(p, z')+F(p-1, 0)]}{A_{44}(z')I_{p-1}[(\bar{m}+z')\xi\gamma^{1/2}]\gamma^{1/2}[(\bar{m}+z')\gamma^{1/2}]^p}\,\frac{1}{F(p-1, 0)\,[F(p-1, z')+F(p, z')]}. \tag{A13}$$

Explicit representations for stress components $\sigma_{\theta z}$ and $\sigma_{r\theta}$ can be obtained from eqns (1) together with $G_{\theta\theta}(r, z; s, z')$ as presented above. The traction Green's function $H_{\theta\theta}(r, z; s, z')$ denoting traction in the θ-direction acting on a plane with unit normal **n** through point (r, z) due to a unit ring load through (s, z') could be expressed as

$$H_{\theta\theta}(r, z; s, z') = \mu_{44}\frac{\partial G_{\theta\theta}}{\partial z}n_z + \mu_{66}\left(\frac{\partial G_{\theta\theta}}{\partial r} - \frac{G_{\theta\theta}}{r}\right)n_r \tag{A14}$$

where n_r and n_z are the direction cosines of the plane under consideration with respect to the r- and z-axes, respectively.